Tunnel Ready Elements for Active Deployment (T.R.E.A.D)

NASA M2M X-HAB 2026 Challenge Final Report

Baldwin Wallace University

Engineering Capstone Team:

Alex Smith, Charlie Woods, Ciaran Smith,

Mike Rodak, Sam Gerber, and Zach Mihok

Faculty Advisors:

Dr. Jeff Dusek

Dr. Jonathon Fagert, P.E.

Sponsored By:

National Aeronautics and Space Administration (NASA)

National Space Grant Foundation (NSGF)

Contents

List of Tables

List of Figures

Executive Summary

The Baldwin Wallace University Engineering Department submitted a project proposal to NASA's Moon to Mars Exploration and Habitation Academic Innovation Challenge (M2M X-HAB). The project goal was for engineering students to design and develop a reusable, deployable tunnel system to facilitate travel between habitats on the Lunar and Martian surfaces. The importance of re-usability is key to preventing the accumulation of buildings and tunnels that no longer serve NASA's purpose and accumulate on the surface. The challenge of these tunnels is to extend and contract fully while also bending and moving along a nonlinear path to dock with other habitats or surface assets. The end of the tunnel must also be able to actuate in six independent degrees of freedom for successful docking. This is due to the high likelihood that the tunnel and habitat will not be perfectly aligned following initial gross tunnel movement; thus, fine control is needed. Our proposed solution to this problem is to combine tendon-based actuation with pressurized bladders for rigidity. The central backbone of the proposed system will serve as the habitable walkway of the tunnel. Therefore, the resistive forces needed to oppose the tendons and cause extension will utilize the bladders embedded into the ribbing/supports of the tunnel. To achieve the necessary bending and movement, a double tendon system is required. The first set of tendons controls the initial half of the tunnel's curvature, while the second controls the final half. Each set consists of four individual cables controlled via a winch system. These tendon systems will also serve as a primary means for retraction. The outer shell of the tunnel is inspired by previous inflatable space projects, but adapts the layers to meet new environmental conditions, updated materials, and preferred mechanical properties. The BW TREAD team evaluated the proposed solution through a small-scale prototype, which was presented to the public during the annual "Ovation" student project day at Baldwin Wallace University.

1 Introduction

For the 2025-2026 X-Hab Academic Innovation Challenge, Baldwin Wallace University investigated soft robotic solutions for a deployable Lunar tunnel. Our focus was on design, fabrication, and demonstration of a 4:9 (by diameter) sub-scale prototype that could extend, retract, and turn for docking purposes while also providing safe travel for astronauts.

1.1 Background and Motivation

NASA's Artemis program aims to establish human presence on the Moon as a stepping stone to Mars. This presence would require structures that could provide safe travel for space personnel between surface elements. Our project addresses this challenge by innovating a soft actuating and deployable tunnel system using a two tendon actuator and a set of inflatable bladders.

1.2 System Requirements

Vision Statement Advance the capabilities and development of inflatable space deployable structures for Lunar and Martian exploration.

Mission Statement Innovate a soft-actuated, deployable tunnel capable of withstanding transit to the lunar environment. Additionally, demonstrate movement capabilities in at least 6 degrees of freedom. This is to aid NASA in the development of human transportation between lunar surface structures.

Problem Statement Design a lightweight, durable, actuatable, and re-deployable temporary structure capable of safely and comfortably transporting humans from one habitat to another without the need for safety equipment.

1.3 Objectives/Requirements

Several objectives were laid out at the beginning of the challenge:

1. The tunnel shall be able to compress for easy storage and transportation. This is both to the lunar surface as well as between uses and when returned.
2. The tunnel shall have an overall weight that is less than the current design weight with linear actuators.
3. The tunnel shall provide an internal environment comparable to atmospheric conditions (15psi) to allow personnel to travel without the use of a space suit.
4. The tunnel shall be able to maintain structural integrity and shape when fully deployed as personnel travel through.
5. The tunnel shall be capable of gross and fine articulation to complete docking procedures.
6. The materials used for the tunnel shall maintain material properties while not in use.
7. The tunnel shall utilize air from reserve air tanks stored within the habitats.
8. The tunnel shall be able to operate using built-in controls within the habitats to minimize external intervention and aid in the extension or retraction process by personnel.
9. The internal habitable space shall be at least 40 inches by 60 inches and extend to 15 feet.
10. Finally, the tunnel shall be able to withstand multiple deployments and operating cycles.

1.4 Project Timeline and Milestones

To apply a systems engineering approach to the design process, our work followed the M2M X-Hab design review schedule:

- System Definition Review (SDR) - October 16th, 2025
- Preliminary Design Review (PDR) - December 9th, 2025
- Critical Design Review (CDR) - February 12th, 2026
- Progress Checkpoint Review (PCR) - March 19th, 2026
- Final Presentation- April 30, 2026
- Final Report May 15th, 2026

These milestones helped guide the progression of our solution. They helped guide the team into groups that tackled different aspects of the project, including inflation, docking, and structural support. Through these presentations, we gained valuable feedback from NASA subject matter experts, which allowed us to grow and develop our solution.

2 System Definition

2.1 Top Level Requirements

The primary design goal is to articulate a system in multiple degrees of freedom to achieve non-tangent docking. Thus, several top-level requirements were chosen for the specific challenges of the tunnel system design. These top-level requirements formed the basis for the flow-down in Figure 1.

1. Compression and Transport
2. Weight
3. Internal Conditions
4. Structural Integrity
5. Docking

Driven by the goals of reduced weight and compact storage, elastic materials must be integrated with the air systems to reduce the overall weight as well as make the tunnel more compact for storage. Another primary design goal is travel without the need for safety equipment. Therefore, consideration of Lunar and Martian environmental effects on the material are paramount to personnel safety. This requires an air control system that ensures internal pressures of the tunnel match those of the habitats to eliminate a pressure difference from one habitat to another. In addition, the structural integrity of the overall system relies on both the inner walkway and the bladders within the rib design. The final part of the system is the docking procedures and operation. With a tunnel made of two independently controlled sections, gross movement and some fine movement are possible. To assist in alignment, the end of the tunnel will utilize a guidance system, such as AprilTags, to reach the other habitat connection point. A flow-down chart for the top-level requirements was created, as seen in Figure 1.

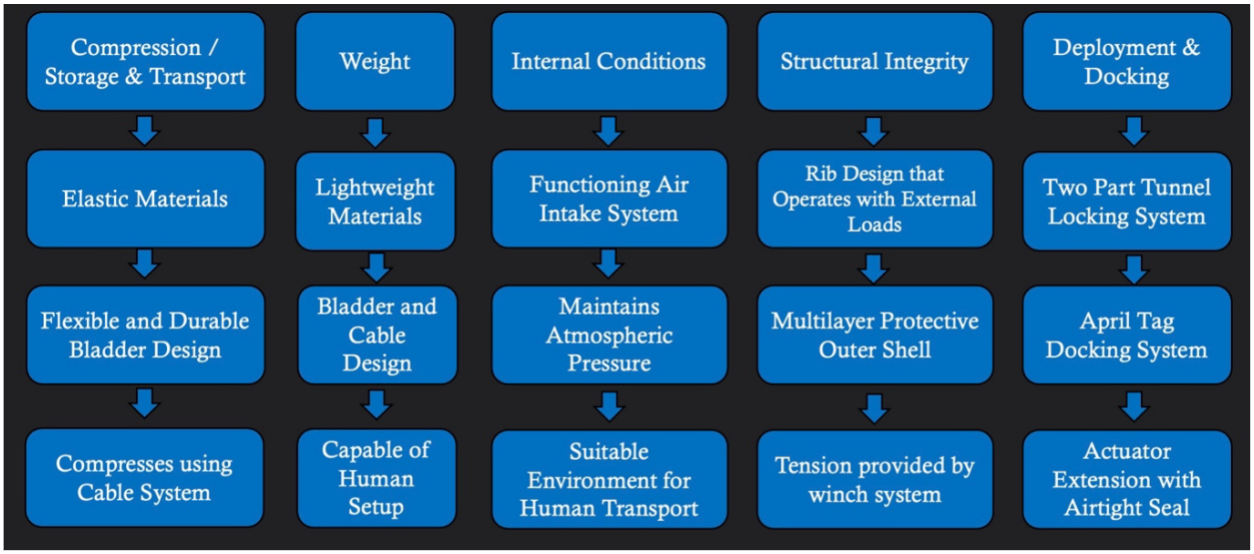

Figure 1: Top Level Requirements Flow Down chart

2.2 System Operations

Looking at the project challenges in Figure 1, the scope was narrowed down to the most important factors. Ideation started with a concept map that considered several articulation possibilities and potential design challenges before beginning the challenge and research. This covered basic requirements such as extension and retraction, along with the potential challenges. Certain topics and/or solutions may be out of the scope of the challenge or could not be tested with current capabilities, but were still valuable to understand. After some deliberation, the potential solutions were narrowed down to focus on retraction, extension/actuation, inflation, and connection. Each one of the main focuses was further broken down into the necessary components and operation procedures shown in Table 1.

Retraction	**Extension**	**Inflation**	**Connection**
Air reclamation system • Valves • Air pumps	Winches used as tension members	Air pumps and valve system to direct air into and out of the tunnel	Redundant gaskets/seals on ends to prevent air leakage
Winches retract cables uniformly • Provide tension for holding in place • Pull tunnel back when disconnected	Guidance system • Distance between ends • Angular relation of ends • Sensor/camera to locate ends	Pressure gauges to ensure guidance pressure and habitable pressure are controlled	Ball and socket joint docking mechanism
Airtight seal on the end		Utilize reserve air tanks within habitats	Mechanical locking system to prevent separation
Durable shell to prevent frictional damage		Work in unison with oxygen tanks	Use of AprilTags to aid docking

Table 1: System Operations

Table 1 was used to further develop insight into a possible testing procedure or solutions needed for a final system to be created. The system utilizes inflation for both the extension of the tunnel as well as the structural integrity. This is achieved via radial bladders to create the structure for the tunnel and provide the resistive force for actuation. The resistance is needed to counter act the tension forces of the cables. Therefore when the cables are pulled, the tunnel turns in the direction where tension is increasing. A general force diagram showing these forces was created (Figure 2). This allows the tunnel to reach the specified docking area and can allow for more complex articulation.

Due to time constraints and technical equipment difficulties, a proper guidance system was not developed for the prototype. However, solutions were discussed such as magnetic ball and socket joints on the end of the tunnel that are guided by AprilTag docking systems. The AprilTags allow

Figure or Table containing sensitive information, or possible unauthorized copyright information has been removed.

Figure 2: System Force Diagram Enhanced With GPT 5.3

the operator to determine distance and angle to the require docking area. The magnetic ball and socket joints will assist with the final alignment. For the retraction of the tunnel, one end must be sealed off and the bladders will deflate while the tendons are wound back into the system. During retraction it is paramount to reclaim the air from the bladders to reduce the difficulty in supplying air for future deployments and reduce the equipment needed.

2.3 Double-Tendon System

To actuate the tunnel, two sets of four tendons run through the outside edges of each rib. The first set of 4 cables will travel from the connection point to the middle section of the tunnel which will control the initial half of the tunnel. The second set of 4 cables will travel from the connection point through the full length of the tunnel. When the first set of tendons is locked and cannot move, the full length cables will only effect the curvature of the second half of the tunnel. In general operations, the first set of tendons would be actuated first. Once the position is achieved, the first set of tendons would be locked in place. Then the second set would be actuated. This allows the tunnel to perform S-shaped curvatures in order to reach and connect habitats that are not face-aligned/parallel in orientation, as shown conceptually in Figure 3 (Left). To explore possible tunnel configurations using a two-tendon system, simulations were performed, as shown in Figure 3 (Right), utilizing functions in the CRVisToolkit [1] from the Continuum Robotics Laboratory [2]. These simulations helped the team understand the capabilities of a two-tendon system and make design decisions about tendon and rib placement.

2.4 Pneumatic Bladders

The bladders are also split into 2 sections, mimicking the setup of the tendons. Two sets of four bladders run alongside the tendons within the rib structure to serve as the driving force for extension. To regulate the pressure and inflation, a series of valves and tubes will provide the bladders with air from an external supply and inflated via an air compressor. Because the tension forces have an impact on the changing internal bladder volume, the bladders must work in tandem with the operation of the tendons. This means the relation between the drag force of the cables and the inflation speed from pressure determines how fast the tunnel extends and how much tension is needed in each cable. Additionally, when fully inflated, the air inside the bladder on the inner

Figure or Table containing sensitive information, or possible unauthorized copyright information has been removed.

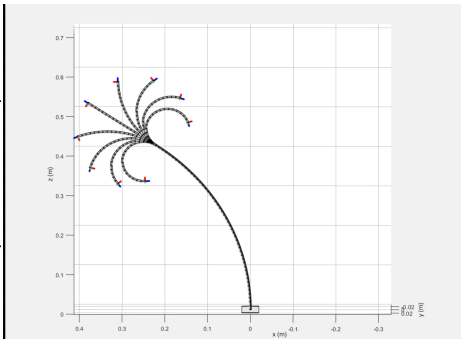

Figure 3: Left: Tunnel Pathing Diagram Enhanced With GPT 5.3. Right: Tunnel pathing simulations.

curvature will have to release air to prevent kinking, while the outer curvature bladders may need more pressure. This will require future experimentation and could lead to predictive modeling in pressure and cable lengths to determine potential pathways.

2.5 Concept of Operations

The Concept of Operations that was developed is as follows: After landing on the lunar or martian surface, the tunnel will either be built into the habitat or be a separate structure that must be attached to the habitat. If designed as a separate structure, a rover or astronauts shall retrieve the tunnel from the delivery craft and take it to an existing habitat. The connection end shall be attached to the existing habitat while the other end stays sealed. Then the tunnel will actuate with a mix of both manual and autonomous control to dock with the secondary habitat. To do this, the tunnels will have cables running through the ribs and attached to winches that retract the cables to actuate the tunnel in the required directions. To actuate the tunnel, the coordination of the other habitat will be placed into a control module. This module will tell the operator the required actuation geometry to achieve connection. This process will be determined by the relationship between cable lengths/tensions and bladder pressures. Once this is done, the tunnel can be deployed with the correct information for pressure, tension, and shape. Near the end of the actuation, AprilTags will be utilized to help guide the final section for controlled fine docking. Finally, once the second end is secured, the inner walkway of the tunnel shall be pressurized from the inside using air from air tanks/compressors on the habitats. After this procedure is completed, the astronauts will be able to travel through tunnels without having to put on spacesuits or safety gear. Once deployment is complete, the tunnel shall be capable of being resealed and retracted to the habitat if needed for future deployments. This is done by deflating the bladders with valves and air reclamation systems. The cables will retract the tunnel structure through the ribs with winches. It is important that these two actions be performed at the same time to prevent bladder rupturing. Additionally, the tunnel should be retracted while straight to reduce the likelihood of kinking. This separates the problem of extending/retracting and bending into two distinct subsystems.

3 Existing Actuation Solutions

To begin developing a solution to the challenge, the team conducted a literature review of academic journals and NASA publications to gain insights from previously published projects. The main focus was looking at the structure and actuation of the tunnels. Three concepts were talked about as possible pathways for a final solution.

3.1 Astromast

For the initial structure of the tunnel, the Astromast was researched and considered for the extension requirement of the tunnel. The idea was pulled from a paper that was revised in 1983 by Peter R. Preiswerk, Laurence A. Finley, and Karl Knapp [3] that looked at large diameter Astromast development. Overall, it is a deployable composite boom that allows for the creation of lightweight, strong structure that can be folded/compressed for launch and then released in space. This technology uses thin-ply composites with multi-directional fibers, making them deformable and suitable for compact storage. The key to this design is the potential energy that is stored in the bent beams when compressed and used to extend later, by releasing the stored energy. These booms are lighter and stronger than traditional metal structures, enabling the deployment of large structures like solar sails and potentially habitats and communication towers on the moon. In addition, this paper describes the attempt to maximize all performance characteristics of a double-laced diagonal Astromast with a diameter of 0.75 m [3]. Looking at the design of the Astromast, this could be innovated to use in the tunnels due to the original compact shape and the ability to extend. However, some drawbacks to the design is that the compressed members are folded into the center of the mast where the potential walkway is.

3.2 Pneumatic Actuators

Looking at the extension and actuation of the tunnel, soft pneumatic actuators were investigated and researched. Since the current design of the proposed tunnels utilized linear actuators which were too heavy, pneumatic actuators would allow for a lightweight solution that covers the necessary requirements. For this, several possible design solutions were explored. Soft actuators, as described in Soft actuators for real-world applications are flexible systems that deform in response to inputs like air pressure, electricity, or other stimuli. They are often made from soft materials such as elastomers. They are commonly used in soft robotics for applications like grippers, wearable devices, and medical tools because they are lightweight and safe to interact with humans. However, while these properties are useful at small scales, there is not much evidence to prove that these systems work at a full scale tunnel large enough for human mobility. The soft actuators rely on material deformation more than structural rigidity, which makes it hard for these systems to maintain stable shapes over long distances and under continuous internal pressure[4].

Fiber-reinforced pneumatic soft actuators were also considered as a possible solution. In a paper written by Joshua Bishop-Moser and Sridhar Kota, fiber-reinforced elastomers were explored, mainly, how the fiber angle accounts for motion control. Elastomer tubes were reinforced with inextensible fibers to control the inflation and direction of the pneumatic actuator [5]. For the purpose of this challenge, this would help create a lightweight solution for the tunnel to be actuated in several degrees of freedom without the use of linear actuators. Depending on the desired position, the fibers could be reinforced at a specific angle to control the direction and extension of the tunnel.

The way that the actuator moves mainly depends on the fiber winding angle, since the fibers control how the material can expand. When the winding angle of the fibers is close to 0 degrees

(vertically aligned), the actuator tends to expand lengthwise because radial expansion is limited. As the angle gets closer and closer to 90 degrees, the axial movement of the actuator is restricted, and the actuator is more likely to expand or bend of the fiber structure is not symmetric [5].

Another example of this fiber reinforced pneumatic actuators was found in the Soft Robotics Toolkit done by the Harvard John A. Paulson School of Engineering and Applied Sciences.[6] This added onto the idea that the motion of the actuators would change depending on how a fiber reinforced actuator is wrapped along with possible strain-limiting layers.

Ultimately, the fiber reinforced soft actuators were dismissed as a solution to the challenge of developing large scale versions. Since the fibers and strain-limiting layers cause different variations in movements, this meant that several different designs would have to be combined to create a possible solution that could be controlled repeatedly. Due to the fact that the tunnels would have to be controlled to several different habitats, the fiber-reinforced actuators would only allow one specific path and would not be ideal for a solution. In addition, the fiber-reinforced actuators are difficult to control and would not allow for the necessary precision in possible docking procedures.

Another possible avenue that was explored was PneuNet actuators [7]. These are a series of internal air chambers embedded within a flexible elastomer. When they are pressurized, the chambers expanded asymmetrically due to the difference in wall thickness or external constraints, causing the actuator to bend in a controlled direction. This design is used mostly in soft robotics because it is lightweight and capable of safe interaction with delectate objects or humans. However, despite the advantages, PneuNet actuators are not suitable for full-scale pressurized tunnel systems. Their structure is designed for localized deformation rather than maintaining rigid or semi-rigid load bearing shapes. Under large scale pressurization the material would experience significant stresses, leading to uncontrolled deformation, loss of structural integrity, or rupture. Additionally, the low stiffness and limited pressure tolerance of elastomer based systems would make it hard to maintain a stable, airtight passage over long distances [7].

3.3 Tendon-based Actuation

Finally, tendon actuation was discovered within the Soft Robotic Toolbox [8]; it is mainly used in prosthetics or claw like robots. It consists of 8 total tendons that run through support ribs that give the system its shape. Another component needed is a backbone so that it has rigidity and the ability to hold shape while flexing in multiple directions. Our system contains six ribs with two sections of four tendons. One section runs the whole length of the tunnel and another only runs halfway. This allows for the tunnel to be bent in two directions at the same time. Our backbone is the walking area of the tunnel, with the amount of pressure needed to support the lives of the astronauts, it can support the tunnel's needs for bending. Figure 4 below shows how the two-tendon system can achieve more complex shapes, which can allow for adaptation to a wider variety of habitat layouts. To extend the tunnel, we are using two sets of air bladders that run half the length of the tunnel. These provide a resistive force to the tendons allowing for the tunnel to be structurally sound. Another component of our tunnel is a durable outer shell that seals off all components from the debris of the environment, while also providing the astronauts protection from radiation and space.

4 System Design

The proposed solution for this challenge consists of a combination of new innovations and inspiration from prior projects and research. The solution is based on a tendon actuation system with special pneumatic bladders for extension and rigidity. The tunnel was designed to meet the

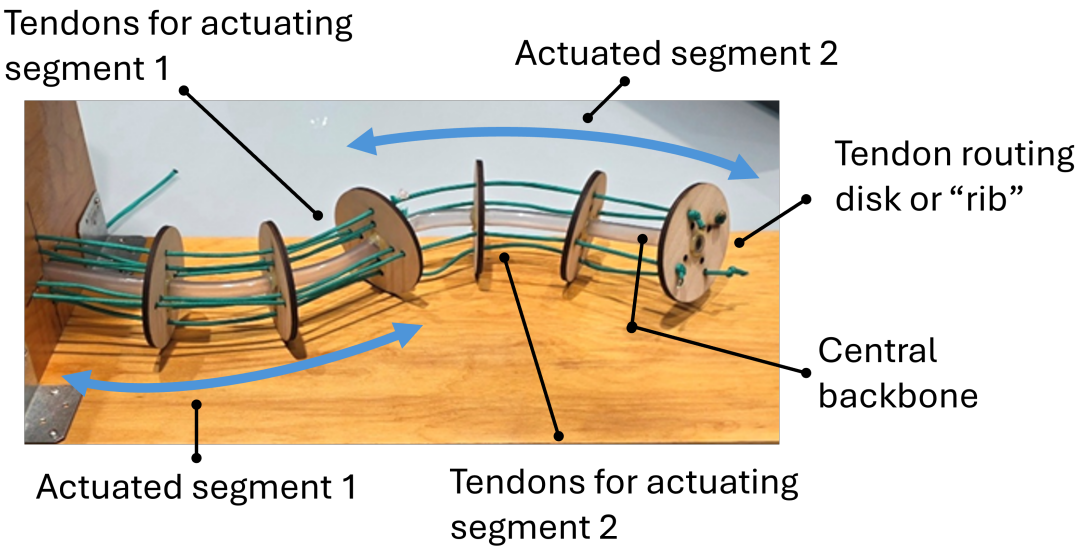

Figure 4: Prototype of a two-tendon actuator showing the system components and independent articulation of each segment.

challenge requirements of a ten-foot length and actuation in six degrees of freedom for docking purposes. The cables will be used for actuation and retraction of the system, while the bladders will be used for extension. The cables will be retracted via winches or a similar system, and the bladder system will be built with an air reclamation system to prevent air loss.

4.1 Tendon Based System

When designing the tendon-based system, the design was kept as close to the original research of having evenly spaced ribs, a backbone, and multiple tendons. Thus, the tunnel will consist of five ribs spaced evenly every 2 feet. These ribs are to be in the shape of 2 concentric circles and be manufactured from lightweight metals such as aluminum or titanium. The sizes of the concentric circles are 9 ft and 6 ft, leaving 3 ft of material around the rib for bladder and cable placement.

The next part of the tendon system is the tendons themselves; the system consists of two sets of four 90° radially spaced tendons. They will be spaced by no more than 6 inches from each other. The material of these tendons could be braided nylon or steel wire. As described before, the first set of these tendons runs the full length of the tunnel, and the other set runs only half the length of the tunnel. The set that runs the full length of the tunnel will be the “outside” set of tendons, while the ones that run half of the tunnel will be the “inner” set of tendons.

The final part of the tendon system is the backbone. The backbone of this system is the walkway itself; it shall be comprised of NASA-inspired materials that are capable of an airtight seal while simultaneously maintaining an atmospheric pressure of 15 psi.

4.2 Pneumatic Bladder System

The pneumatic bladder system is primarily for the extension and stability of the tunnel. This system will consist of 2 sets of 4 bladders, with their pressures being individually controlled. The 2 sets of bladders will each run one half of the tunnel for better air regulation and improved actuation curvature. The size of the bladders will be 1 ft in diameter while being 5 ft long. The material

for the bladders should be similar to the materials used in the Trans-Hab Space Station built by NASA. These bladders should be able to hold a minimum pressure of 2.2 psi for elongation and a working pressure of 5 psi for actuation, based on initial calculations. The spacing of the bladders should be 90 degrees radially while being spaced 45 degrees radially from the tendons. Each of these bladders should have its own regulator that controls its pressure. These regulators need to be remotely controlled as they will remain inside the tunnel structure. Lastly, based on the curve of the tunnel, the bladders need their pressures adjusted to withstand the stress that is put on them.

4.3 Outer Shell

The outer shell shall consist of layers of fireproof insulation, bladder material, Kevlar, and radiation shielding to protect against the environment in space and on the lunar surface. The size of the shell shall be at least 10 ft long with reinforced material along the locations of the ribs. The outer diameter of the shell is unknown due to the different environments between open space and the lunar surface. However, it was noted that the overall thickness will be much thinner as there are fewer concerns on the surface compared to open space. For reference, the Trans-Tab shell was approximately 18 inches thick to protect against micro meteoroid impacts and major temperature swings. Regarding temperature swings, the tunnel insulation must maintain a temperature of around 70 degrees Fahrenheit. The external materials chosen must withstand the Lunar regolith and should be able to rub against the surface without major damage. Additional consideration and research were made for the buildup of charges on the lunar surface. A simple grounding system can be used to discharge this built-up charge.

4.4 Walkway Floor

The floor of the system has been considered heavily; however, due to time constraints and focus on critical components, a final walkway was not included in the presented prototype. Some potential solutions were investigated, and the most promising took inspiration from a playground. Some playgrounds have bridges that consist of a tension system that uses diagonally braced rods/cables. These rods/cables would be placed inside the ribs with tension members attached to them. These members would run down to floor level and come together in a flat-bottom “V” shape. A segmented floor would then run over top of these members to allow for safe travel of the astronauts and other objects that need to be moved. Figure 5 below shows an example of the playground rope bridge walkway that serves as inspiration for the notional solution.

Figure 5: Interior Walkway Inspiration

5 CAD Models

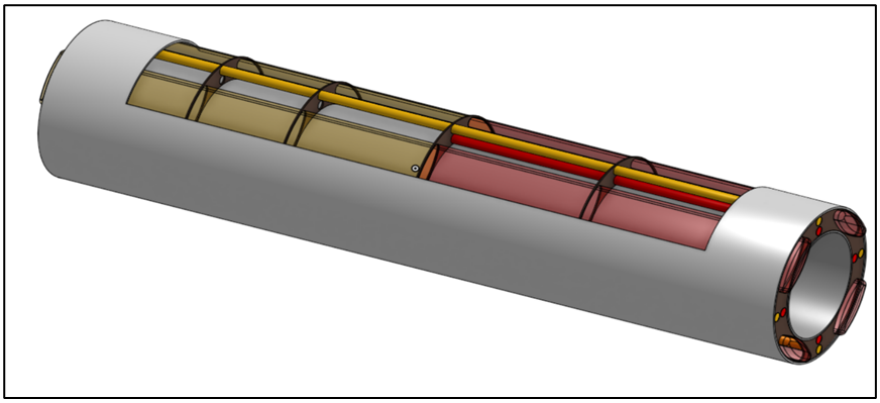

Figure 6: Full Two Tendon System CAD Model

This is a model of the full two-tendon system; the yellow and the red translucent objects are the bladders that split the tunnel. The yellow and red tubes are the tendons that operate the system. The gray is the outer shell with a cutout for an inside view, and the brown objects are the ribs that support the system.

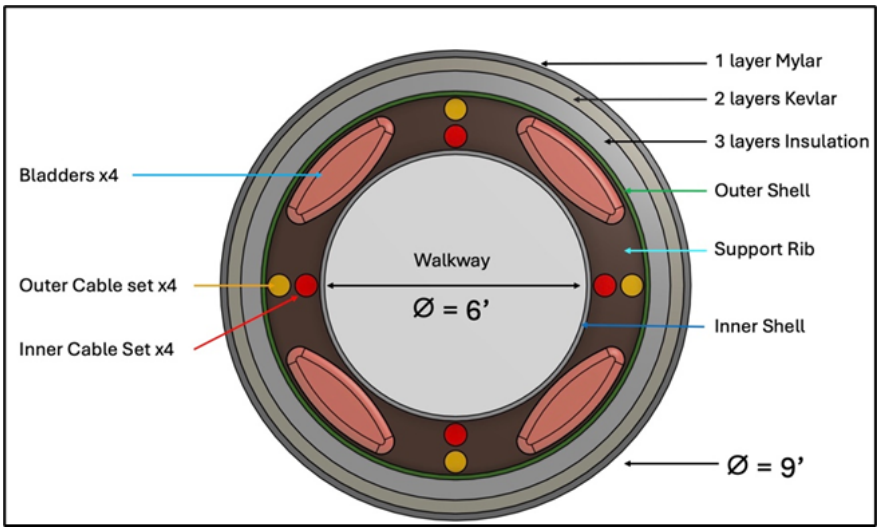

Figure 7: Cross Section View of Tunnel

This is a cross-sectional view of the same system, but further developed. Now, a more protective layering system has been added to the shell. In addition, dimensions have been set for the system where the inner diameter is 6 feet, the outer diameter is 9 feet, and the tunnel length itself is 10 feet.

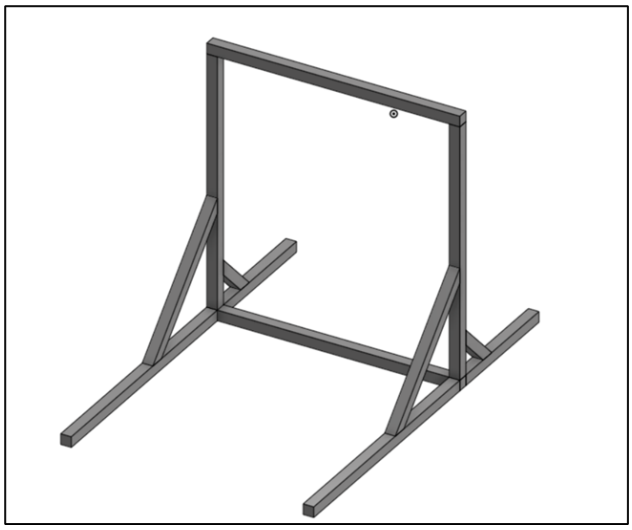

Figure 8: Prototype Frame Assembly

The model shown here is the frame assembly for the final prototype. This is constructed from 80/20 1-inch aluminum and was designed to prevent the tunnel from rolling over on itself. The initial frame is 4 ft x 4 ft, with the 4 support legs being 4 ft and 2 ft respectively. The cross members are 2 ft and 1 ft sections cut at a 45º angle.

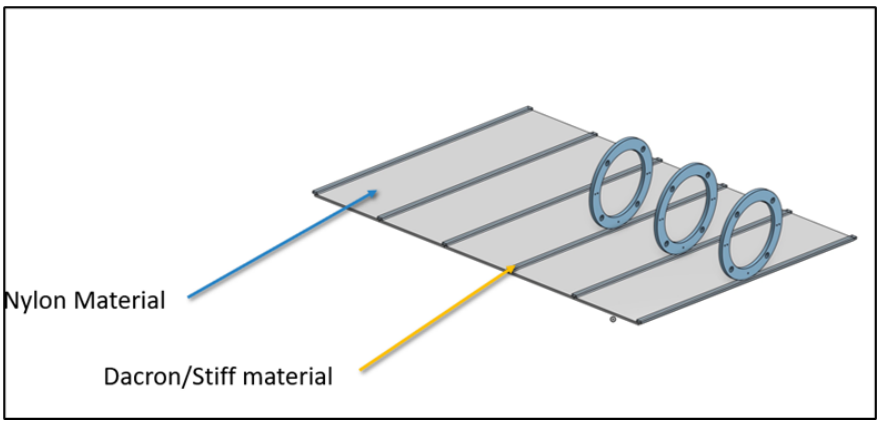

Figure 9: Prototype Shell Design

The model above is the shell design for the final prototype. It is made from ripstop nylon similar to that of a boat sail. There are strips of Dacron sewn evenly into it for attaching to the support ribs. The model is a 14.5 ft x 15.5 ft rectangle that was eventually taped together to form a cylinder.

6 Risk Analysis

Operating on the lunar surface poses several technical and environmental risks, especially for a system intended to enable personnel to travel without a spacesuit. Because the system must maintain a controlled internal environment, even small failures could lead to severe consequences. Several risks were considered, and a plan, summarized in Table 2, was developed to address the more critical risks of the system.

The primary risk involves the air containment system. Potential leaks may occur due to improper sealing between the tunnel and habitat, material fatigue, or damage to the internal bladders. For this, a multi-layered design and reliable sealing procedures are necessary to maintain structural integrity and pressure. Another concern is the lunar environment, particularly the lunar regolith and electrostatic charging. The Regolith particles can accumulate in mechanical components and air systems. This may cause premature wear or failure. Also, static charge buildup from the surface may affect system performance. For this, grounding systems may be used, such as a grounding sheet or circuit, and protective outer layers to prevent the regolith from entering mechanical components.

There are also structural and mechanical risks. These include the durability of the floor materials, such as support ribs under repeated use, weight distribution, and possible effects of reduced gravity on the tendon-based actuator systems. Addressing these concerns requires careful selection of the materials used, testing under simulated loads, reducing the friction between components, and the use of lightweight components. There could also be a possibility for replacement plans. This ensures that the system is not in use if a component reaches failure, as well as limits for the components. The limits would indicate when components are not strong enough for deployment, but this component failure does not mean complete failure for the system.

Looking at the lunar environment, problems arise in the form of extreme temperatures. Large temperature swings between the lunar day and night can possibly affect actuator performance. There may need to be thermal management strategies.

System performance risks related to actuation and pressure differences must be evaluated. Since the actuator relies on pressure differentials, testing in vacuum-like conditions is needed to ensure proper functionality. In addition, scaled testing of mass and load conditions can further validate the design before implementation. This includes testing until failure to understand the weaknesses, as well as being able to add a factor of safety or redundancies to the system.

7 Proof-of-Concept and Material Selection

Throughout this project, several experiments were conducted. Most of these were proof-of-concept experiments, which are not meant to determine whether the experiment passes or fails. Rather, they are designed to see if there are characteristics that could be utilized and applied to the final solution. Overall, this section covers the analysis, design concepts, and testing of these small-scale prototypes of the proposed system. Additionally, this section will delve into some of the experiments conducted on the subsystem design ideas used in the final prototype.

7.1 Initial Proof-of-Concept Prototype

The first proof-of-concept experiment was conducted based on two different questions and looked at four different characteristics. Since the bladder and cable system was recently proposed at this point, experimentation was done to see if a compact tunnel could be extended and retracted using

Item at Risk	Description	Likelihood	Risk Level	Mitigation Strategy
Bladders	Bladders fail to fully inflate due to leaks or material degradation	Medium	High	Use space-rated, durable bladder materials, testing until failure, possible leak detection
Cables	Cable system wears during repeated deployments or tie off system fails & lose tension	Medium	Medium	Use durable cables, figure out how and when they will fail, cable replacement plan, try not to operate if cables fail, retract and repair
Shell Material	Outer material wear over time due to contact with lunar surface or inner material wear from travel	High	High	Specify high strength materials, seals where necessary, reduce friction and wear/unnecessary damage to materials
Retraction System	Tunnel materials, bladders, or cables are affected by uneven retraction	High	High	Deliberate folds to retract the same each time, set up into straight position before retraction

Table 2: Risk Management Plan

the bladder cable system, and if a scale model tunnel could be actuated vertically and horizontally by the cables. The characteristics to look at were the ideal shape of the support ribs, bladders, cables, and other materials in the experiment that could be applied to prototypes, as well as iterate on possible problems.

The initial proof-of-concept experiment prototype used a wood backing board that would act as a “habitat” (where the model would be fixed), and then the cables and bladders would run through the wood backing. Several support ribs were manufactured from a hardboard and laser cut to size. Each support ring has four holes, 90 degrees radially from each other, with one hole in the middle for a bladder. Eventually, the bladder was to be wrapped with material to decrease the chances of it popping, as well as aiding in the extension. The success metrics for the experiment were that the tunnel shall extend 20 inches from a compressed state, it shall be capable of an 8-inch horizontal movement from a center line, the tunnel shall be capable of lifting the free end to a minimum of 6 inches, and the tunnel shall fully retract to the original compressed state or within 2 inches. The CAD models for the experiment are shown below in Figure 10.

The rings measured 4 inches in outer diameter with a 2-inch inner diameter for the bladder. The two sets of cables were attached to the center and end ribs, respectively, and the ribs were evenly spaced at roughly 3 feet to avoid extending without adding support.

The initial bladders used for the first proof of concept experiments were party balloons. The balloons were preferred due to the shape needed, being inflatable, and being cheap. However, due

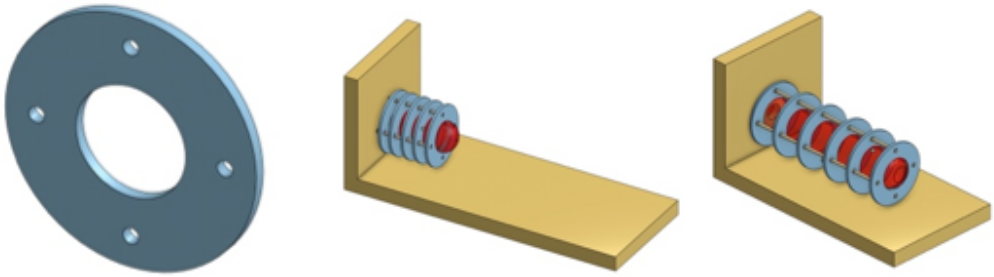

Figure 10: Proof of Concept CAD Models

to the thin walls and friction with the tunnel, the balloons were prone to popping. This led to a series of iterations for the bladders to find a material that would be usable for the proof-of-concept experiment. The other materials tested were trash bags, plastic fabric, and a paint tarp. The trash bag was flexible but was not durable, and could not produce any successful results. The plastic fabric was durable and could hold air, unlike the trash bag, but it was too thick to the point where it would not create a smooth curvature. The thick fabric would kink in one spot when articulated by the cables, causing it to be very difficult to form into the desired shape. On top of this, it also had a lot of trouble compressing. The paint tarp worked better; it shaped easily and was durable enough for the experimentation. However, it did not seal well, and it was difficult to set and seal the air valve in place.

Overall, the experiment provided great characteristics and feedback to take into the following prototypes and experiments. For bladder materials, the material needs to be thick enough that it will not burst when pressure is applied, durable enough to last several deployments, but flexible enough to create smooth curves to decrease the force put on the bladder and the rest of the tunnel. The cables were able to provide actuation of the tunnel in one direction at a time, and only a single curve was horizontally achievable. Due to the problems with the bladders, only one shape for the support rib was tested, which was a circular cross-section. Some additional shapes that were considered were triangular and half-circle cross-sections to allow for more stability. However, the timing constraints prevented these shapes from being tested, but they would be good next steps in future iterations.

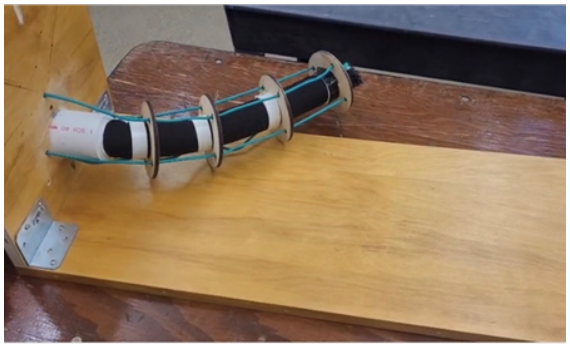

Figure 11: Initial proof-of-concept prototype. The results from this experiment informed future design requirements and helped support system design decisions.

7.2 Double Tendon Model

The second iteration of the tendon system, shown in Figure 12, incorporated two sets of four tendons. One set of 4 ran the entire length of the system, while the other ran only half. This allows for an "S" shaped curve, as one set can pull in one direction while the other can pull in the opposite direction. The central backbone of this prototype was a rubber tube to independently test the complex curvature capabilities of this design. What was achieved by this prototype was the proof that the double tendon system could be used to achieve the lateral and horizontal degrees of freedom needed. The only draw back it that the degrees of freedom are codependent on each other as the entire length of the tunnel moves with the end rib, which changes with more curvature.

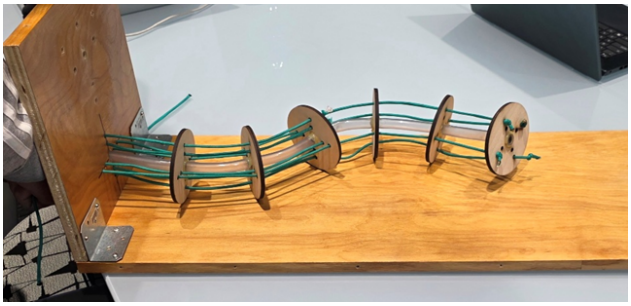

Figure 12: Double Tendon Prototype

7.3 Inflation System

Latex Flex Hose

Initial searches for bladder materials focused on air-tight materials that could expand laterally and not radially when formed into a tube shape. Thus, the first test was done of a self-expanding garden hose that had a durable outer woven layer and a flexible inner rubber lining. Believing this could be a perfect small-scale replicate of what was desired overall for the tunnel, a section of hose was connected to the air system. After the pressure in the hose matched the system, there was no visible extension. The hose could extend once assisted by hand, but did not meet the requirements of self-expansion. It is believed that the failure was due to the original purpose being for water, not air, which led to a rupture at the valve connection.

Polyurethane Bladder Stiffness Research and Experimentation

After multiple proofs-of-concept with faulty bladders, the team pivoted to doing further research into more durable bladder materials. The challenge here was finding elastic materials that would remain durable when in use, while also conforming to a long cylindrical shape with a small diameter. Initially, the thought was to use kite-board bladders as a model and see how they performed, given that kite-boarding bladders are made from polyurethane, which can elongate while still staying rigid when in use. Additionally, the polyurethane bladders would be able to inflate to the small cylindrical shape needed because of their customization, and they are a commercially viable option. Other considerations for materials included Latex, due to its high elasticity being beneficial in tunnel articulation, Combitherm film, because of its usage in aerospace applications, and catheter balloons, for their small compact size and their input/output tubes allowing for easy access for air supply.

From here, the task became researching different properties for each of the previously mentioned materials, with the main categories being modulus of elasticity, modulus of rupture, and tensile strength. These were the chosen properties because of their overall impact towards how the bladder would perform under high pressures and frequent expansion and compression, which would have a significant affect on the performance of the bladders. Additionally, the thickness of each material was collected to examine the potential impact of material thickness on internal air pressure. During the research phase, the assumption was that the standard materials of Nylon 12 and Pebax 6333 would be used for materials involving the catheter balloons, as well as natural latex being represented. Additionally, for the Combitherm, a similar material with more readily available material properties was used, specifically the material Victrex Peek 450GL30. These findings were compiled in Table 3 below.

Material	Thickness (mm)	Inner Diameter (mm)	Elastic Modulus (GPa)	Modulus of Rupture (GPa)	Tensile Strength (GPa)
Polyurethane [9], [10]	0.09	76.11	0.05	0.022	0.65
Nylon12 (catheter) [11], [12]	0.02	76.18	1.8	1.59	0.0593
Pebax6333 (catheter) [13], [14]	0.02	76.18	0.24	0.285	0.053
Combitherm [15], [16]	0.14	76.06	11.5	11.0	0.185
Natural Latex [17], [18]	0.254	75.95	0.05	0.0017	0.005

Table 3: Bladder Material Mechanical Properties

Combitherm had the highest Modulus of Elasticity at 11.5 Gigapascals. For the highest modulus of rupture, Combitherm had the highest value of 11 Gigapascals, as well as the highest tensile strength with 185 Megapascals. This initially led to the thought of the Combitherm being the desired material, given its dominance with the material properties; however, the issue found with the Combitherm was its availability for use, since obtaining space-grade Combitherm, as well as the substitute material, Victrex Peek 450GL30, is out of the financial scope of this project. After deciding not to go with the Combitherm, the tensile strength factor became negligible because of the closeness in values, leaving either the polyurethane bladders or the Nylon 12. Ultimately, the decision came down to what the prioritization was, leading to the polyurethane bladders being chosen for their elastic capabilities, which would bode well with the tunnel's focus on articulation.

7.4 Tunnel Analysis and Actuation Design

With the bladder material now selected, the thought became how the bladders would behave when subjected to stresses when the tunnel is actuating and if the chosen material will be able to withstand these stresses. Knowing how much resistance the bladders will be able to endure from

stresses when the tunnel is in use became a priority because if the bladders are not able to handle the stresses then they could potentially kink or rupture. Having a way to quantify this resistance to applied stress led to the idea that since the inner and outer diameters already being known, the moment of inertia could be found with its respective Equation 1, allowing for this resistance to stress to be found. The moment of inertia allows for the moment about the end of the bladder to be solved for, this matters because as forces are applied to the bladder, the bladder will want to bend, and knowing how much the bladder could bend would be useful in determining the amount of stress permitted. In order to calculate for this moment, the moment of inertia would be multiplied by the modulus of elasticity for that material.

$$I = \frac{\pi \left(D^4 - d^4\right)}{64} \tag{1}$$

The idea was to treat the bladders as cantilever beams with a point load occurring at the end of the bladder, representing the tensile force from the tendons. These forces would be solved by experimenting with various values for the sum of moments about the fixed end of the bladder. The goal of this process is to gain a more comprehensive understanding of the total deflection and movement capable of the tunnel. Knowing the theoretical capabilities and limitations of the tunnel can help with modeling potential path shapes using the radius of curvature for each of the two sections. This method of modeling is for a simplified model of the tunnel, however, it also came the assumption that the tunnel would have a fixed end at the source habitat, and that the tension in the cables act like an applied moment at the end of tunnel. To solve for the radius of curvature, Equation 2 could be utilized where “R” is the radius of curvature, “M” is the generated moment about the end of the bladder, “E” is the modulus of elasticity of the desired material, and “I” is the moment of inertia from the bladder [19].

$$\frac{1}{R} = \frac{M}{EI} \tag{2}$$

Both the concepts of deflection and radius of curvature are shown in the image below, with deflection being denoted by “h” showing how far the line has moved vertically, and the radius of curvature being a circle that best approximates the curve from the line, denoted by “R”.

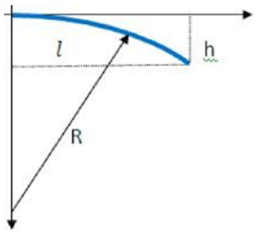

Figure 13: Radius of Curvature

The challenge that arose from using this method was that the flexure rigidity is dependent on pressure, and a theoretical expression for the current model is not readily available for the kite boarding bladders. This led to the decision that the stiffness of the bladders would need to be determined experimentally.

7.5 Experimental Determination of Bladder Flexural Rigidity (EI)

Testing started by inflating a polyurethane bladder until there was enough air to make the bladder firm, but without deforming it. The bladder was then measured and marked at its horizontal halfway point with tape, 45 inches, with half of the bladder secured to the table, and the other half overhanging and free to move. As a result, the bladder could be modeled as a 1 m long cantilever beam. One person held the end of the bladder on the table, while the other person recorded the deflection. Multiple meter sticks were taped together so that they lay flat overhanging the surface of the table and that they were parallel with the bladder. The surface of the table served as the reference for the x-axis of this experiment, with the distance above and below the overhanging meter sticks being the y-axis. A ruler was then put against the meter sticks to measure how far down the bladder would deflect away from the x-axis. An example of the experimental setup is shown in Figure 14 below.

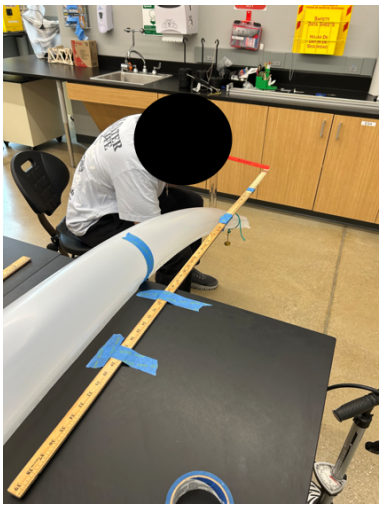

Figure 14: Bladder Deflection Experiment

During testing, a string was tied around the extending end with a hanging mass that would increase during each run-through of the experiment. After each weight was added, the vertical deflection of the bladder was measured and recorded. The weights that were added during the experiment were measured in grams to better understand smaller changes in forces exerted on the bladder before considering how the bladder would operate with larger forces. Table 4 below summarizes the results of this experiment.

Force (N)	Deflection (m)	Experimental EI ($N \cdot m^2$)
0	0.0254	0.00
98.1	0.0762	429.13
196.2	0.1016	643.70
294.3	0.127	772.44
392.4	0.1524	858.27
490.5	0.1905	858.27
588.6	0.2286	858.27
686.7	0.2794	819.26
784.8	0.3175	823.94
882.9	0.381	772.44
981	0.4394	744.20

Table 4: Flexural Rigidity Experimental Results

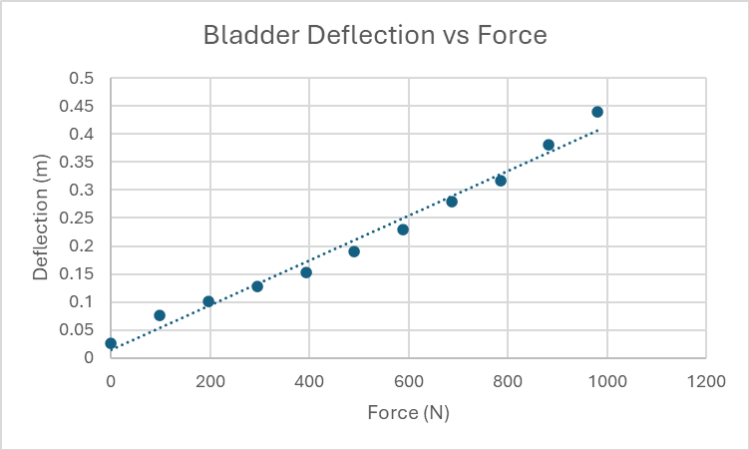

Figure 15: Experimental results for the bladder deflection experiments. The slope of this line is inversely proportional to the effective flexural rigidity of the bladder, *EI*.

From the table, the deflection remains consistent with 1-inch increments for every 10 grams of weight added, aside from at 50 grams, where there is a 1.5-inch increment. At 80 grams, the deflection begins to deviate, and the increments become closer to 2.5 inches. Figure 15 visualizes this behavior with there being a sudden increase and immediate decrease between 0 Newtons and 200 Newtons, and then the points remain linear until 800 Newtons is applied, and the data points appear to become more positively exponential. This change from linear to exponential happens when 80 grams is applied, which is due to the bladder beginning to kink and having a harder time supporting itself upright. The behavior at the beginning, with sudden increases and decreases on the graph, could be from human error when running the experiment. Overall, the bladders are very reactive to tensile forces, but now knowing how much force could be exerted without kinking, parameters could be set for the tendons to not risk loss of structural rigidity of the tunnel. The data collected through this experiment was then used to calculate an experimental "EI" value, or the flexural rigidity of the bladder.

This was achieved through using the equation based off of a cantilever beam with a point load at the opposite end and a fixed end for support, but reworked to solve for the flexural rigidity value. Equation 3 below shows the theoretical behavior of the beam. In this expression, δ is the vertical deflection, P is the applied force, l is the length of the beam, and EI is the flexural rigidity. To experimentally determine the value of EI for the pressurized bladder, this expression can be reworked so that the "EI" term is isolated, the independent variable is the point load P, and the dependent variable is a multiple of the recorded deflection. The ensuing relationship is shown in Equation 4 below [20].

$$\delta = \frac{Pl^3}{3EI} \tag{3}$$

$$\frac{3\delta}{l^3} = \frac{P}{EI} \tag{4}$$

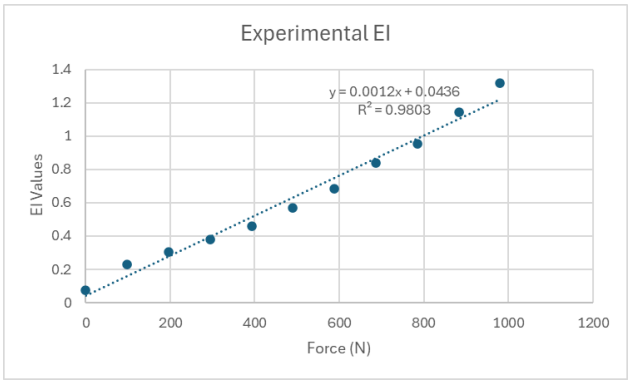

Figure 16: Experimental EI values compared to Exerted Forces

These modified values can then be plotted, and the slope of the best fit line for this data is equal to $\frac{1}{EI}$. Figure 16 shows this transformed data and the best fit trendline. The experimental flexural rigidity value is calculated by dividing the slope, 0.0012, by 1, yielding a value of $833.33 Nm^2$. This value can then be used as a basis for analyzing the behavior of the tunnel.

7.6 Tunnel Actuation Modeling

With an experimental value for the flexural rigidity, the actuation of the prototype tunnel can now be modeled. Like before, the tunnel can be reasonably approximated as a cantilever beam. The tension in the cables exerts an eccentric load on the tunnel, causing rotation (moment). As such, the overall deformation can be modeled as a cantilever beam with an applied moment at its end. This deformation expression is shown in Equation 5 below. In this expression, the value of the moment, M is obtained by taking the tendon tensile force, and multiplying it by its perpendicular distance from the center of the tunnel (specified as 0.5334m in the prototype), $M = Force * 0.5334$. Note that, in this formulation, the total flexural rigidity of the four bladders is approximated as the individual EI multiplied by four. Future work can explore how the four pressurized bladders interact with each other, or how applying differential pressure affects this overall "EI" value.

$$\delta = \frac{ML^2}{2EI * 4} \tag{5}$$

Similarly, the radius of curvature can now be calculated by taking the experimental flexural rigidity value and multiplying its value by four to account for all of the bladders, then dividing that quantity by the moment. Knowing the radius of curvature allows us to know how sharply the tunnel will bend when in use. Equation 6 below shows how the radius of curvature, R can be calculated for a given applied moment, M, and flexural rigidity, EI.

$$R = \frac{4 * EI}{M} \tag{6}$$

By establishing a relationship between the applied tensile force, the radius of curvature, and the deformation, the range of motion for the tunnel can be determined. Table 5 shows an example of these calculations. In this table, when a tensile force is applied to one of the tendons, the resulting expected deformation and associated radius of curvature can be calculated. These calculations were performed assuming a tunnel length of 4.5m. As can be seen from this analysis, for the prototype, it is anticipated that relatively low tensile forces (order of magnitude 100-600N) can be applied to achieve reasonable deformation (as much as 1m). In operation, this could be used in reverse; if the location of the destination habitat is known, the desired deformation/radius of curvature can be determined, and the necessary tensile load calculated.

Tension (N)	Moment ($N \cdot m$)	Radius of Curvature (m)	Deformation (m)
110	58.67	56.81	0.18
120	64.01	52.08	0.19
130	69.34	48.07	0.21
140	74.68	44.64	0.23
150	80.01	41.66	0.24
200	106.68	31.25	0.32
300	160.02	20.83	0.49
400	213.36	15.62	0.65
500	266.70	12.50	0.81
600	320.04	10.42	0.97
650	346.71	9.61	1.05

Table 5: Theoretical Applied Tension vs Tunnel Deformation

8 Final Tunnel Prototype

Using the lessons learned from the proof-of-concept experiments and materials selection, a final tunnel prototype was constructed, as shown in Figure 17. The final prototype was a 4:9 sub-scale model (by diameter) of the proposed final design with dimensions given in Table 6. To support the tunnel and represent the habitat, a frame was constructed from 80/20 T-slot aluminum, as shown in the left frame of Figure 18. The prototype tunnel incorporated the double tendon system discussed in Section 7.2 with prestretched braided dacron rope for the tendons (#550 dacron leech line). As shown in Figure 18, the rope tendons passed through 3D printed brackets that held the ribs to the T-slot aluminum frame and prevented them from cutting through the ribs. These ribs were fabricated from fiberglass-reinforced foam, which were chosen for their lightweight and structural properties, as shown in Figure 20. Details of the rib design, testing, and fabrication are provided in Section 8.4.

	Length (ft)	Tunnel Inside Diameter (ft)	Tunnel Outside Diameter (ft)	Number of Ribs
Full-Scale Tunnel	10	6	9	5
Final Prototype	15	2.5	3.5	6

Table 6: Comparison of Full-Scale and Final Prototype Tunnel Dimensions

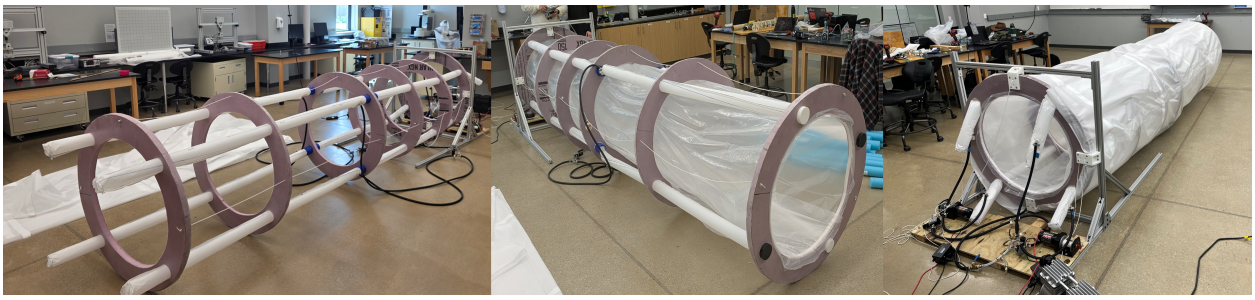

Figure 17: Evolution of the final tunnel prototype. Left: The fiberglass-reinforced foam ribs supported by pressurized bladders. Middle: Plastic sheeting added to the tunnel to serve as internal walls. Right: Final tunnel prototype with nylon outer shell.

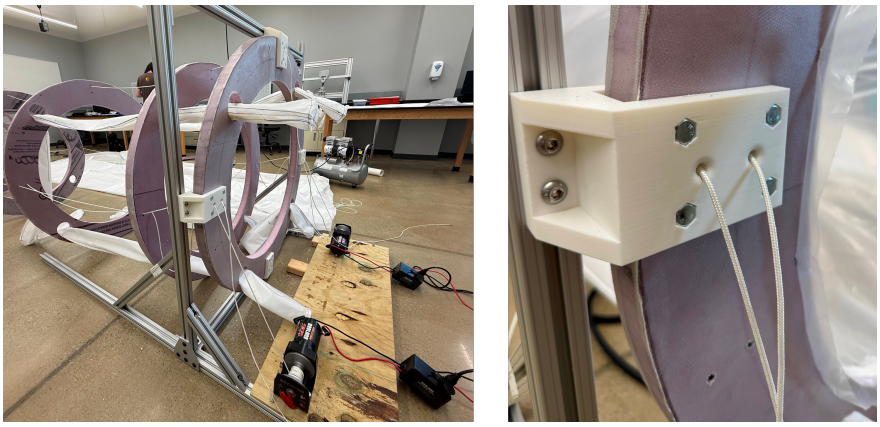

Figure 18: Left: Electric winches were used to control tension in the outer tendons on the left and right side of the tunnel, providing lateral articulation (sway). Right: Braided dacron tendons passed through 3D printed brackets to prevent cutting through the fiberglass-reinforced foam ribs.

For actuation, the prototype utilized electric winches (Badland ZXR 2500 lb. ATV/Utility Winch) on two of the tendons. The winches were powered with a 12 volt automotive battery and controlled via push button remotes, as shown in Figure 18. The decision was made to restrict winches to two tendons to manage prototype cost while proving the viability of the tendon-based actuation at a larger scale than the proof-of-concept experiments. The winches were also used to demonstrate the retraction of the tunnel, as shown in Figure 24. The tunnel was extended, as shown in Figure 25, using thermoplastic polyurethane (TPU) film bladders enclosed in 1.5 ounce ripstop nylon sleeves, as discussed in Section 8.1. The bladders and nylon sleeves are shown clearly in the left frame of Figure 17 before the inner and outer tunnel surfaces were added. The bladders were pressurized using an electric compressor and pressure regulators (Norgren Modular Compressed Air Regulator, Series R82, 4-30 PSI), as shown in Figure 19. Details of the air management system can be found in Section 8.2. A bill of materials for the prototype is provided in Appendix A.

8.1 Prototype Bladder Design

For the prototype, the diameter of the bladders needed to be determined because the strut kiteboard bladders were tapered, and the decision had to be made if the bladders were to remain tapered or if they should be constrained by a sleeve so that a set diameter could be maintained. The bladder sleeve was used because the if the bladders were left unconstrained they would have expanded too much to fit in the ribs, so then the team needed to find the smallest diameter of the bladder and constrain them to that size. This diameter was found to be 2.5-inches, but we decided to make the bladder sleeve 3-inches to allow for some tolerance because of the high amount of internal pressure that will be in the bladder. The sleeves for the bladders were to be made from ripstop Nylon material because of the high modulus of rupture, as well as the material being very cheap and accessible from a local sailmaker. With a set diameter for the bladders, a cross-sectional area was calculated out to be 0.00456 m^2. The next step was to move into some baseline calculations to determine roughly how much force would be required to get the tunnel to extend outwards with the use of the bladders. To determine this, an approximate weight of the tunnel was needed, which was thought to be 450 Newtons based on the size and shape of the outer shell, materials and components, the number of ribs, and weight of the fully inflated bladders. A coefficient of static friction of 0.6 was used for the concrete floor that the tunnel would be pushing against [21]. From here the static frictional force equation was used to calculate the force required for movement, with N representing the force from the weight of the tunnel, and μ_s representing the static coefficient of friction.

$$F = \mu_s * N \tag{7}$$

The total amount of force that would need to be exerted from the four bladders was found to be 270 Newtons, which is about 60 pounds-force, or about 15 pounds-force from each bladder. Following this the required pressure necessary in a bladder to achieve extension was calculated by taking the required force in each bladder, and dividing that value by the cross sectional area of the bladder itself. A summary of these calculations is shown in Table 7. This concept can be adapted for Lunar or Martian applications to determine the required pressure for extension.

Movement Force Calculations	
Static Friction Coefficient (outer shell to concrete)	0.6
Tunnel Weight (N)	450
Required Force for Movement (N)	270
Force per Bladder (N)	67.5
Required pressure for bladder extension (Pa)	14801.38
Required pressure for bladder extension (psi)	2.15

Table 7: Movement Force Calculations

8.2 Prototype Air Management System

Now having a solid basis for the tensile forces for the cables, the pressure for the bladders, and the theoretical deflections, the focus shifted towards developing a functional air intake system. The thought going into designing this system was that the air running to the first set of bladders needed to be controlled separately from the second set of bladders. Having this in mind, the air intake system was also meant to try and control each of the bladders as individually as possible. The finalized design for the air intake system, as shown in Figure 19, mostly accommodates for both of these criteria by being able to control the first set of bladders independently from the second set, while being able to dictate the flow of air to bladders in pairs, with the Top Left (TL) and Top Right (TR) controlled by a regulator (R), and the Bottom Left (BL) and Bottom Right (BR) controlled from a different regulator. To ensure that the first set of bladders was independent from the second set, two ball valves are used to operate the air flow for each set as needed, with one ball valve controlling air to the first set and the other controlling the air to the second set, with the air for the system coming from a portable air compressor.

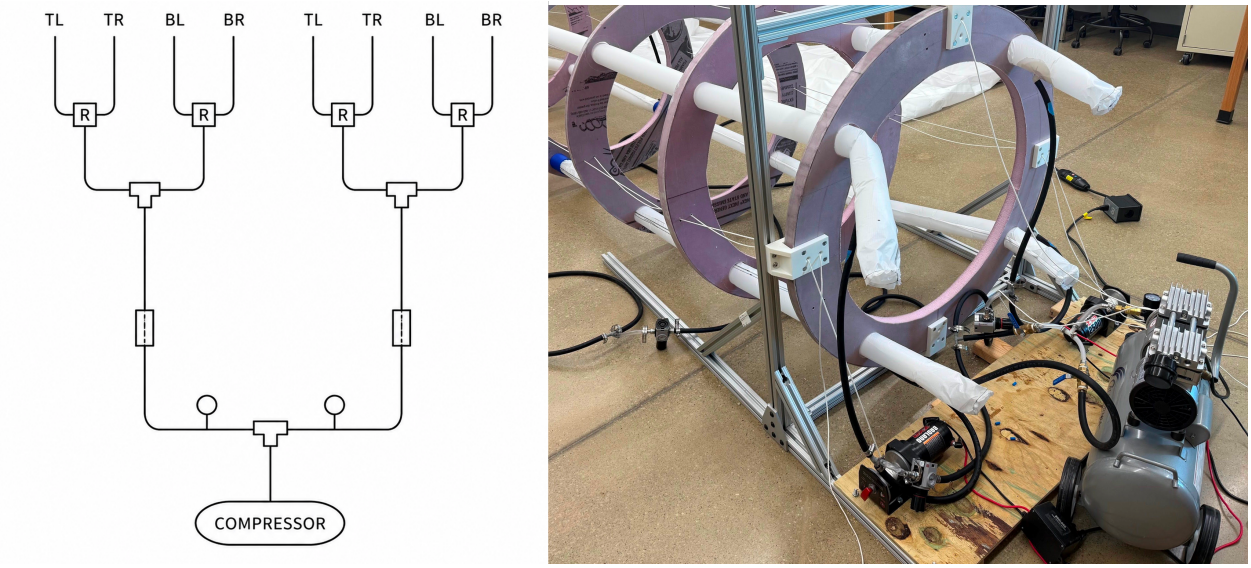

Figure 19: Left: Diagram of the air management system denoting regulator (R) and valve placement. Right: Air management system on the final prototype.

With the air intake system design finalized, it was then constructed by cutting a rubber air hose to different lengths for the tubing, then attaching the 4 regulators with ¾ inch barbed fittings. T-hose fittings were used to separate the top two bladders from the bottom two bladders, as well as to direct the air flow to the two ball valves, as shown in Figure 19. Once assembled, the air intake system will enable fine-grained control and monitoring of the pressurized bladders. Each regulator had to be set, and the process involved starting off by turning on the air compressor, but with both ball valves closed. The air compressor then had to have its air flow set with its own regulator, which was kept on the lower end, going no higher than 20-30 psi to reduce potential risks. From here, the regulators for the bladders were then to be adjusted from 0 psi to a desired psi based on how quickly the air was traveling into the bladders and by the stiffness of the bladders. Through

experimental findings, the optimal range to set the 4 regulators for the bladders was found to be between 5 and 7 psi. This pressure range proved favorable, with the bladders inflating at a steady rate until they were sufficiently pressurized for structural support for the tunnel. This observed value during operation was around 5 psi, which validates the lower end of the calculations.

8.3 AprilTags

As mentioned, the chosen method to aid the docking procedure was AprilTags, which is an open-source 3D camera detection system using patterns similar to QR codes. AprilTags are used in conjunction with detection libraries, like OpenCV, that can be downloaded on a computer, commonly a Raspberry Pi, where 3D data, like position, distance, and angle, is output. To use these to aid the docking of the tunnel, the tags are to be displayed at the desired docking location, and a camera is to be attached to the very end of the tunnel and connected to the Raspberry Pi. This will relay back to the start of the tunnel, giving a position reading and how far the tunnel must go or turn, depending on the complexity of the code.

Despite the potential benefits of using AprilTags as part of the tunnel system, there were several complications that were encountered while experimenting with them. First was the issue of working with libraries that were not compatible with the current version of Raspberry Pi. Then, it was found that official Raspberry Pi cameras work best for AprilTag detection. After these roadblocks were dealt with and the camera was detecting the tags, all that was left was changing the code so that the angle could be output. For the Raspberry Pi to detect the angle of the tag, the camera needs to be calibrated so that its parameters can be found, which is a very complicated and lengthy process. This proved more difficult than expected and ultimately caused the AprilTag system to be excluded from the final prototype.

8.4 Rib Manufacturing and Testing

For the support ribs, the BW TREAD team evaluated three different foam boards. The three boards were as follows: 1.5” thickness Foamular NGX High Performance XPS Insulation from Owens Corning (pink), 1.5” thickness EPS rigid foam insulation from Henry R-tech (white), and the same for the 2” thickness. A layer of fiberglass sheet would be layered on top of each side and a 5:1 ratio two-part epoxy (TotalBoat Traditional 5:1 Epoxy) would be used to seal the fiberglass. Due to the timeline and possible lack of epoxy, only the 1.5” pink foam and 2” white foam were fabricated and tested. Each foam board was cut to size as one solid piece of foam with a 4 foot diameter. One side of each foam board was layered and allowed to cure. After 3 days, the fiberglass and epoxy were applied to the other side.

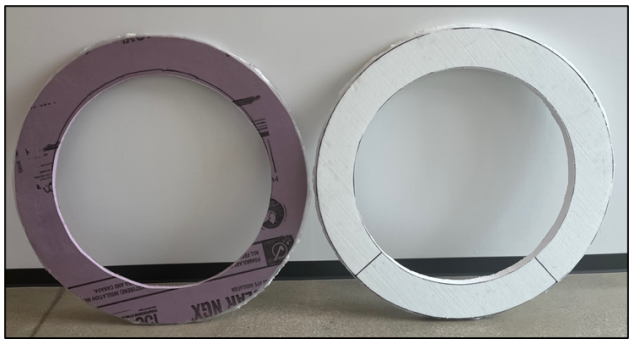

Figure 20: Cut out of foam board for ribs

8.5 Testing Process

To test the fiberglass ribs, a basic deflection/bending test was done to determine which foam board would be best for the final prototype, as shown in Figure 21. Because of some of the time restrictions, the bending test was a time-effective way to help determine which foam board was best. Both of the ribs had fiberglass on one side. The fiberglass side was placed halfway on a table, facing up. For each of the tests, more weight was placed on the furthest part of the ribs to see how much deflection and mass each rib could hold. Both of the ribs were tested until failure, then rotated 90 degrees and tested again. A meter stick measured the distance from the ground, and a measurement was made again after each weight was placed on to measure how much the rib was bent. The results are shown in Tables 10 - 13 in Appendix B.

Overall, the white foam performed better than the pink foam but there was not a huge difference in strength. All of the tests on the ribs failed where the ribs were placed on the edge of the tables (which is logical as it is the location of highest bending moment/stress). In addition, the manufacturing process for the pink foam was much easier to lay up fiberglass as well as cut out the necessary holes. Looking at the failure for the two foam ribs, the pink foam bent and dropped the weights. However, the foam board did not completely crack, opposed to the white foam that completely cracked in half, rendering it unusable. Because the pink foam was able to hold around the same weight as the white foam, that failure of the pink foam meant that it was still able to hold its shape. For this reason, on top of the ease of manufacturing, the pink foam board was chosen for the prototype.

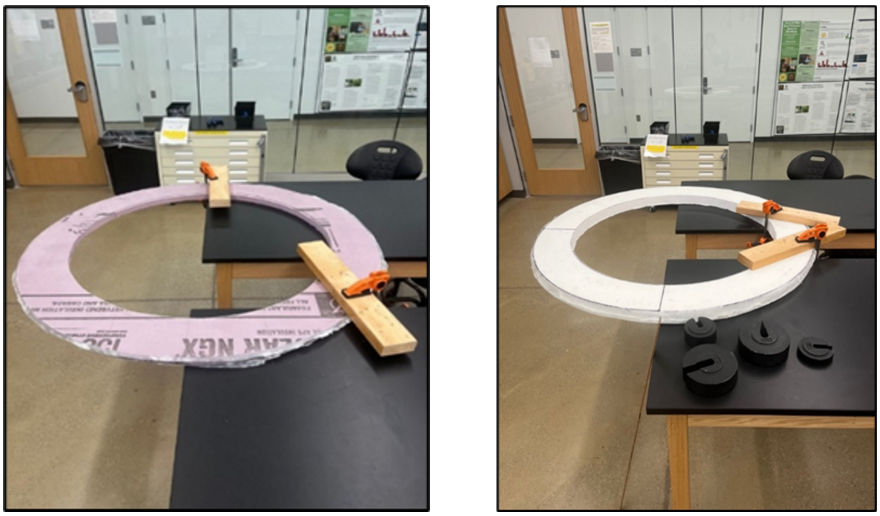

Figure 21: Testing the strength of fiberglass-reinforced foam for use in tunnel ribs.

After further information on the forces put on the ribs by the tendons was obtained, additional testing was done on the pink rib. For this test, four pieces of wood elevated the foam rib, as shown in Figure 22. The placement of the wood was to mimic the bladder placement on the rib. Since the pink foam ribs failed in four spots radially 90 degrees apart, that is where the ribs were supported by the wood. Weight was added to the three spots where the cables would go for the prototype to test if the ribs were strong enough to withstand the forces that would be placed on them by the cables. The deflection was measured the same way from one of the points on the rib. The pink rib testing deflection test results are shown in Table 14 in Appendix B.

Figure 22: Pink foam stress testing

From the testing, the pink foam never reached absolute failure, meaning the point where the foam is not usable. Instead, it deflected enough that it could not hold the weight anymore, which happened when the applied mass was 24 kg (approx. 52.91 lbs.). Based on the calculations described in Section 7.6 and results in Table 5, these tests support the notion that approximately 0.32m of deformation could be achieved before rib failure was a concern. This could be further mitigated in future design iterations by using a larger rib at tendon attachment locations. This test was completed with the pink foam with fiberglass only on one side, and the foam had already been tested. For the final prototype, the pink foam had fiberglass applied to both sides as well as the outside edge.

8.6 Final Prototype Layup Process

With the size of the boards from The Home Depot, the diameter of the pink foam was reduced by an inch to utilize as much pink foam as possible. With the initial diameter, only one support rib was able to be manufactured from a sheet. With the reduced diameter, two ribs could be manufactured. Measurements were marked on the foam boards for the outer and inner diameters of the support ribs, and the outer diameter of the ring was cut using a bandsaw. Once all support ribs were cut, the fiberglass was laid on one face of the support ribs as well as the outside of the ribs. After the epoxy for the fiberglass had time to dry, a Dremel was used to cut off the excess fiberglass, and the edges were sanded down to aid in adherence. The second face of the support ribs, as well as the edges, was reinforced.

9 Results & Analysis

To test the performance of the double tendon actuation system, the tunnel was extended and the outer full-length tendon was retracted using one of the electric winches (shown in Figure 18). The horizontal deformation of the tunnel end was recorded as a function of tendon retraction distance, as shown in Table 8 and Figure 23. Results demonstrated that after an initial pretension of the tendon, the deformation of the tunnel end was linearly proportional to the amount of tendon retracted. While the magnitude of deformation aligned well with the predicted values in Table 5, additional experiments with a load cell on the tendon would be beneficial. Extension of the tunnel was also verified, shown from left to right in Figure 25, and retraction was tested to verify a compact stowed position for transport and storage, as shown in Figure 24.

The results from operational testing of the prototype were successful actuation in 5 of the 6 degrees of freedom: surge, sway, heave, pitch, and yaw. All of the linear degrees of freedom could actuate; however, the 2 axial degrees (pitch and yaw) were difficult due to the lack of pressure in the bladders, as well as only two winches controlling the lateral movement. This could be a limiting factor as the first section of the tunnel had to be operated by hand. This could impact the overall operation of the tunnel by not having a constant force being applied to the cables or being locked in place. Overall, the winches are able to hold the cables in place, locking the position of the entire tunnel into one curve.

Looking at the compression of the prototype (Figure 24), by retracting both winches and manually retracting the top cable, the prototype was able to compress and stand on its own within 1.5 feet. Following the compression, the valves for the air system were opened, and the winches were slowly released to extend the tunnel, as shown in Figure 25. Fully inflated, the tunnel reaches a final length of just over 13.5 feet.

Length of Tendon Retracted (m)	Length of Tendon Retracted (in)	Horizontal Deformation (m)	Horizontal Deformation (in)
0.08	3	0	0
0.15	6	0.37	14.56
0.23	9	0.52	20.47
0.30	12	0.74	29.13
0.38	15	0.9	35.43
0.46	18	1.19	46.85
0.53	21	1.29	50.78
0.61	24	1.38	54.33
0.69	27	1.45	57.08
0.76	30	1.56	61.41

Table 8: Tunnel Actuation Test

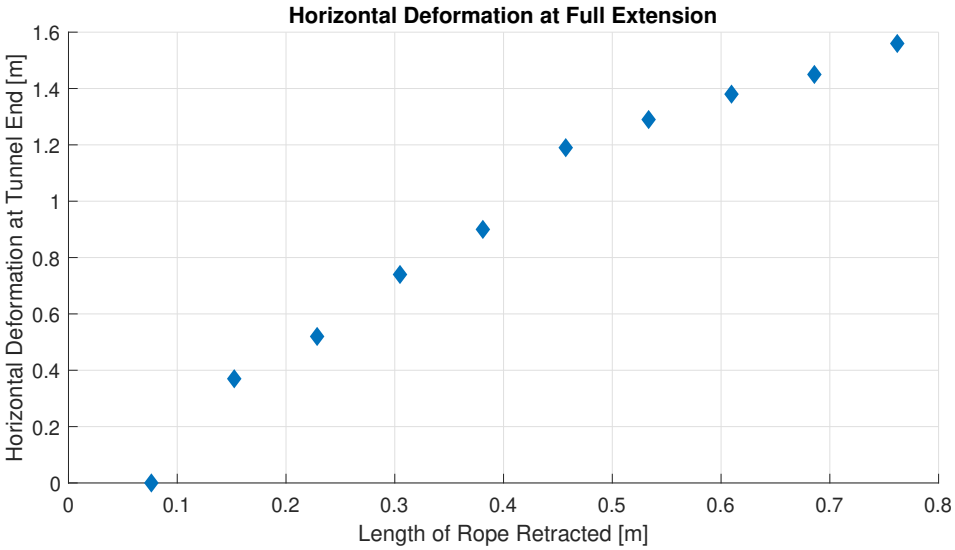

Figure 23: Amount of rope retracted by the winch system compared to the horizontal deformation at the end of the prototype tunnel

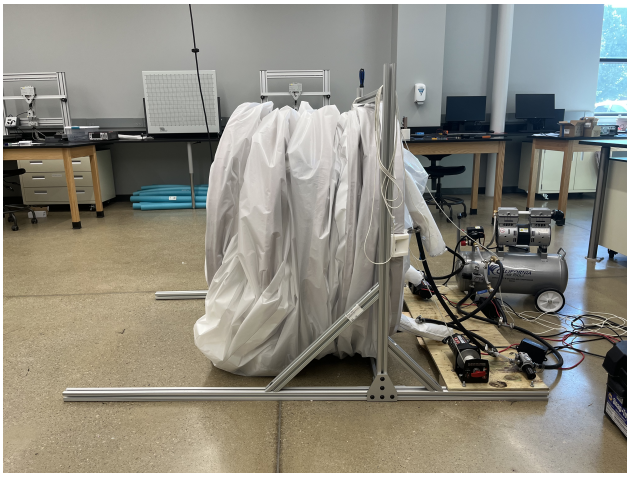

Figure 24: Prototype Compressed Position

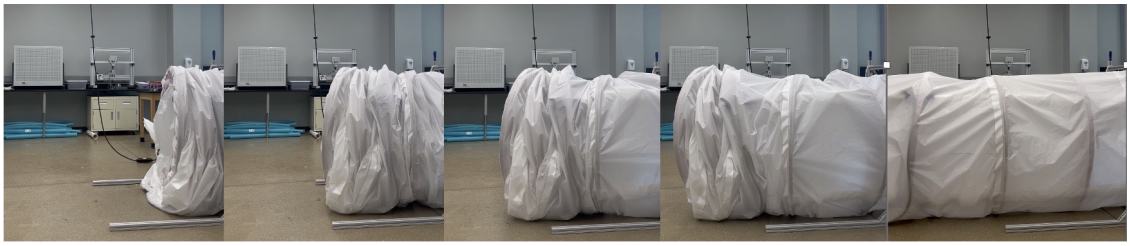

Figure 25: Prototype Extension Process

10 Summary and Next Steps

In conclusion, the research and proposed solution provide valuable information for a possible continuation of this system. The BW TREAD team achieved articulation in 5 of 6 degrees of freedom with the final prototype tunnel. Articulation in roll was not pursued in the development of the final prototype, but could be achieved in the future through approaches such as helical tendons or active rotation of the tunnel root. The current prototype adds additional information for successful future outcomes. Through proof-of-concept experiments as well as a scaled prototype, the two-tendon system was demonstrated to be a viable option to actuate a tunnel. The material characteristics discussed provide an outline for bladder and shell options to scale and continue the prototype process. Through assembly and manufacturing it was learned that the bladders are the most important part of the system. The materials that make the bladders, as well as the material that encases them, must be able to withstand several deployments, pressures up to 15 psi, and be elastic enough to curve with the actuation of the tunnel while maintaining pressure. These bladders were the largest challenge for the team. Even though the polyurethane bladders have particular characteristics that were needed, a lack of a manufacturing process for bladder sleeves, and the inability to withstand or maintain enough pressure over several deployments means that these bladders specifically are not a viable option moving forward, however bladders manufactured to the exact size and made with a material able to sustain high pressures, are the solution for this design. Future design iterations would search for a similar material but with mechanical properties that better align with system demands. The cable system has proved to work in proof-of-concept experiments as well as in qualitative tests with the final prototype. Due to the friction of the cables with the support ribs, the cable holes must be reinforced to mitigate the risk of wearing overtime. The fiberglass support ribs have maintained their strength through the current testing, but due to time involved in the manufacturing process, alternative means should be looked into to maximize the effects of a composite rib design. With the information provided, the BW TREAD team believes that a tendon and bladder system is a possible solution given more time, budget, and continued testing and research.

10.1 Next Steps

While working on this challenge, other ideas and concepts were considered, but were either out of the project scope or were cut due to time constraints. One solution included wheels that are attached to the tunnel, which work in the same way as a movable soccer goal. These wheels would provide stability for the tunnel and make it easier to move and operate via a lever-lifted wheel base. Attached to each of the wheels would be a servo motor that pulls the lever and flips the wheel onto the ground, allowing it to roll. Another idea for the rotation aspect of the 6 degrees of freedom was to install a worm gear system at the end of the tunnel. A toothed gear attached to the inner side of the outer shell and a corresponding worm gear are turned by a motor at the end of the tunnel. Unfortunately, due to time constraints, this was not tested or investigated further. Additional ideas for rotation were possibly adding a 3rd set of cables that run the length of the tunnel but are integrated in a helix pattern along the ribs. This would wind the cables around the tunnel and, when retracted, would cause the tunnel to roll its entire length. This could be explored further in future design iterations.

Another direction for future development involves the proposed AprilTag-based docking system. Preliminary design with an AprilTag system suggests that it could be used to facilitate fine-

grained actuation at the docking location. The BW TREAD team attempted to implement a scaled version of the system, but, due to unforeseen technical issues, was not able to complete it. Moving forward, future design iterations could experiment with their use and explore how they can assist with final docking.

The bladders themselves could have gone into further testing and refining, with one potential idea being considered was to to use a vacuum chamber to experiment with the kite boarding bladders and simulate how they might operate in areas with conditions similar to the Lunar or Martian environment. This idea was ultimately not utilized because of the lack of time as well as not having readily available access to a vacuum chamber. Other areas of interest with the bladders would have been to further develop the air intake system so that there could be a way to release from a given set of bladders, allowing for more potential geometries from the tunnel to be achieved. This idea, while incredibly useful, did not happen because of the planning and component wait times involved with the air intake system. The shape of the bladders is an area that could be expanded upon with the idea of "bellow" shaped bladders being a potential consideration. The bellow shape would allow for the bladders to compress in a more uniform manner when the tunnel is retracting, and could help mitigate kinking in the bladders. While this idea did generate interest, the decision to test the bladders as a rigid body with the uniform shape they had in the final prototype was done so that a baseline understanding for how the bladders behave in response to stresses could be made.

With the tunnel utilizing multiple different systems in its design, that being the air intake system for the bladders and the winches for the tendons, the thought was that a way to build on these systems would be to automate them. A control station would be used for making more precise measurements for these systems. The user would input values for the desired geometry of the tunnel, and then the control station would read these inputs and send set amounts of air into each of the bladders so that the bladders would be able to be more rigid or relaxed as need be. The control panel would also control the winches by regulating how much of the cable is reeled in so that the winches would pull the tunnel into the desired geometry and apply the appropriate tensile force in the tendons. This control panel would be ideally in the starting habitat. This idea could also tie back into the April Tags by having the camera system transmit live footage back to the control panel. This also led into the idea of having various controllers incorporated into the panel to oversee the various systems as a manual way to dictate the articulation in the tunnel. This would be through means of having the air intake system being regulated by various valves controlling each bladder, and the winches being controlled by buttons that would either have the winch pulling or releasing the cable. Ultimately, the control panel was not looked into further because of the time limitations that would come with designing such a system as well as continuing work on the tunnel itself.

10.2 Community Educational Outreach

As part of the outreach program of the capstone project, several opportunities were discussed. After some deliberation and schedule availability, it was decided that the BW TREAD team would participate in the Score with STEM outreach program hosted by the NEOSTEM Ecosystem and the Cleveland Cavaliers at the Rocket Mortgage Field House in Cleveland, Ohio. Several tables of system prototypes and an informational poster about the current state of the project were displayed. Figure 26 shows TREAD team members presenting their preliminary work to attendees. Approximately 500 students from several surrounding schools participated in the event, with ages ranging from elementary to high school. During the 4-hour program, demonstrations of the double tendon

actuation approach were provided using the proof-of-concept model shown in Figure 12, and many discussions about both the university and the capstone project were held. Both the team and the project's faculty advisors helped with the demonstrations to the attending students. Although the event was to promote the future and interests of engineering overall, there was definitely some success in sharing the work being done by NASA and what plans are being made for the future, along with the need for the next generation of engineers.

Figure 26: Members of the BW TREAD project team discuss their tunnel concept at the Score with STEM educational outreach event.

References

[1] Continuum Robotics Lab, *CRVisToolkit: A Visualization Toolkit for Continuum Robots*, https://github.com/ContinuumRoboticsLab/CRVisToolkit, 2023.

[2] Continuum Robotics Laboratory. "Continuum Robotics Laboratory at the University of Toronto. "[Online]. Available: https://crl.utm.utoronto.ca/.

[3] P. Preiswerk, L. Finley, and K. Knapp, "Large diameter astromast development, phase 1," Tech. Rep., 1983.

[4] M. Li, A. Pal, A. Aghakhani, and M. Sitti, "Soft actuators for real-world applications," en,

[5] J. Bishop-Moser and S. Kota, "Design and modeling of generalized fiber-reinforced pneumatic soft actuators," *IEEE Transactions on Robotics*, vol. 31, no. 3, pp. 536–545, 2015.

[6] *Tendon-driven continuum robots with extensible sections—A model-based evaluation of path-following motions - Ernar Amanov, Thien-Dang Nguyen, Jessica Burgner-Kahrs, 2021*. Accessed: Feb. 26, 2026. [Online]. Available: https://journals.sagepub.com/doi/10.1177/0278364919886047.

[7] M. S. Xavier et al., "Soft Pneumatic Actuators: A Review of Design, Fabrication, Modeling, Sensing, Control and Applications," en, *IEEE Access*, vol. 10, pp. 59 442–59 485, 2022, ISSN: 2169-3536. DOI: 10.1109/ACCESS.2022.3179589. Accessed: Sep. 15, 2025. [Online]. Available: https://ieeexplore.ieee.org/document/9785890/.

[8] J. B. Kahrs, *Tendon Driven Continuum Robots*, en-US. Accessed: Feb. 26, 2026. [Online]. Available: https://crl.utm.utoronto.ca/_pages/tdcr.html.

[9] Y. Zhou et al., "Fabricating core-shell co@c/PLA/TPU composites via fused deposition modeling for synergistic electromagnetic absorption and mechanical enhancement," *Materials Science and Engineering: B*, vol. 330, p. 119 518, Aug. 1, 2026, ISSN: 0921-5107. DOI: 10.1016/j.mseb.2026.119518. Accessed: May 5, 2026. [Online]. Available: https://www.sciencedirect.com/science/article/pii/S0921510726003454.

[10] "Tpu material datasheet," Tech. Rep. [Online]. Available: https://www.basf.com/dam/jcr:19c11827-1bc0-3b0f-a3f4-4fc2b986d54f/Elastollan_Properties-Physical-Properties.pdf.

[11] "Nylon 12 technical data, mechanical, thermal, electrical properties," Accessed: May 6, 2026. [Online]. Available: https://www.k-mac-plastics.net/data/technical/nylon-12.htm.

[12] "Engineering plastic nylon 12," Tech. Rep. [Online]. Available: https://www.smithmetal.com/pdf/plastics/nylon-12.pdf.

[13] "Pebax6333 data sheet," Tech. Rep. [Online]. Available: https://www.sushengpolymer.com/media/pdf/kuvEwW_Pebax-6333-SP-01.pdf.

[14] "Pebax 6333 polyether block amide pellet data sheet," Tech. Rep. [Online]. Available: https://www.hongrunplastics.com/public/uploads/images/20251010/ARKEMA%20PEBA%20PEBAX%206333%20SP%2001.pdf.

[15] "Victrex peek450gl30 material datasheet," Tech. Rep. [Online]. Available: https://www.materialdatacenter.com/mb/material/pdf/481570/481570/VICTREXPEEK450GL30.

[16] "Victrexpeek450gl30 material datasheet," Tech. Rep. [Online]. Available: https://www.spacematdb.com/spacemat/manudatasheets/Victrex_TDS_450GL30.pdf.

[17] L. S. says. "Properties of natural rubber — learnbin." Section: Rubber Technology, Accessed: May 6, 2026. [Online]. Available: https://learnbin.net/properties-of-natural-rubber/.

[18] A. Arulrajah, M. M. Disfani, H. Haghighi, A. Mohammadinia, and S. Horpibulsuk, "Modulus of rupture evaluation of cement stabilized recycled glass/recycled concrete aggregate blends," *Construction and Building Materials*, vol. 84, pp. 146–155, Jun. 1, 2015, ISSN: 0950-0618. DOI: 10.1016/j.conbuildmat.2015.03.048. Accessed: May 6, 2026. [Online]. Available: https://www.sciencedirect.com/science/article/pii/S0950061815002950.

[19] "Elastic bending theory - roy mech," Accessed: May 8, 2026. [Online]. Available: https://roymech.org/Useful_Tables/Beams/Beam_theory.html.

[20] "Beam design formulas with shear and moment diagrams," Tech. Rep. [Online]. Available: https://engineering.purdue.edu/~ce474/Docs/DA6-BeamFormulas.pdf.

[21] "Coefficients of friction for concrete - the physics factbook," Accessed: May 8, 2026. [Online]. Available: https://hypertextbook.com/facts/2006/MatthewMichaels.shtml.

A Prototype Bill of Materials

Materials & Supplies		Hardware & System Components	
Item	**Qty**	**Item**	**Qty**
Party Balloons for Bladder Testing	1	Nylon Tee Fitting	1
Trash Bags for Bladder Testing	1	Brass Ball Valve	2
Thick Plastic for Bladder Testing	1	Polyethylene Tube	1
Paint Tarp for Bladder Testing	1	T-Slot Frame (24”)	2
Wood	n/a	T-Slot Frame (12”)	2
Nylon Strings	n/a	T-Slot Frame (2 ft)	2
PVC Pipe	n/a	T-Slot Frame (4 ft)	6
Balsa Wood	3	Corner Bracket for Frame	8
3/4” Barb Insert	8	Surface Bracket for Frame	2
Hose Clamps	1	Double Nut Pack	5
Pocket Hose for Bladder Testing	1	Triple Nut Pack	1
Epoxy Card Spreader	1	L Connector Valves	10
Epoxy Kit	1	Bladder Shipping	1
Epoxy Aluminum Roller	1	Poster Printing for Community Outreach	1
Hazmat Fee	1	Respirator Filters	2
Tendon Winches	2	Respirators for Fiberglass Layup	2
Final Prototype Strut Bladder	10	Vapor Cartridge	1
Barb Adapter	4	Air Hose (ft)	60
Single Nut Pack	2	Air Regulator	4
Frame Mounting Bracket	4	Filter Brackets	4
T-Hose Fitting	6	SS Bolts Pack	1
Zinc Barbed Fit	8	Impulse Sealer for Bladder Customization	1
Diverter Valve	1	Sealer Shipping	1
Foam Boards for Rib Fabrication	3	Air System Shipping	1
Brushes for Epoxy Layup	6	Brass Adapter	4
Hole Cutter for Rib Fabrication	1	Brass Valve (alt)	2
Zinc Bolts	16	Carpet Tape	1
Zinc Nuts	16	Double Tape	1
Clear Sheet for Tunnel Interior	1	#505 Dacron Leech Line for Tendons (ft)	150
Ripstop Nylon for Bladder Sleeves	1	1.5 oz. Rip-Stop Nylon Roll (yds)	8
Sail Tape for Sleeve Repair	1	Adhesive Dacron (yds)	1

Table 9: Project Bill of Materials and System Components

B Fiberglass-Reinforced Foam Rib Testing Results

From ground to bottom of ring = 88 cm		
Weight (kg)	**Deflection (cm)**	**State**
1	1	Good
2	2	Good
5	3.5	Good
7	5	Good
10	Failure	Failure

Table 10: Deflection Results for Pink Rib

From ground to bottom of ring = 87.5 cm		
Weight (kg)	**Deflection (cm)**	**State**
1	0.7	Good
2	1.5	Good
5	2.5	Good
7	2	Good
10	4	Good
11	4.5	Good
12	5	Good
15	Failure	Failure

Table 11: Deflection Results for White Rib

Rotated 90 degrees after first failure		
From ground to bottom of ring = 88 cm		
Weight (kg)	**Deflection (cm)**	**State**
1	1.5	Good
2	3.0	Good
5	4.5	Good
7	6.0	Good
10	8.0	Some Cracking
11	Failure	Failure

Table 12: Deflection Results After Rotation 1.5” Pink Rib

Rotated 90 degrees after first failure		
From ground to bottom of ring = 88 cm		
Weight (kg)	**Deflection (cm)**	**State**
1	1.0	Good
2	2.0	Good
5	3.0	Good
7	3.5	Good
10	5.0	Some Cracking
11	5.5	Good/Cracking
12	Failure	Cracking Then Broke

Table 13: Deflection Results After Rotation 3" White Rib

Weight (kg)	**State**	**Deflection**
1	Good (No Cracking)	0.25
2	Good (No Cracking)	0.50
4	Good (No Cracking)	1.00
5	Good (No Cracking)	1.25
6	Good (No Cracking)	1.50
7	Good (No Cracking)	2.00
8	Good (No Cracking)	2.25
9	Good (No Cracking)	2.50
Moved to Water Buckets		
10	Good (No Cracking)	2.25
11	Good (No Cracking)	2.25
13	Good (No Cracking)	2.50
14	Good (No Cracking)	2.50
17	Good (No Cracking)	2.75
18	Good (No Cracking)	2.75
19	Good (No Cracking)	2.75
21	Big cracks	3.50
22	Small Cracks	4.00
23	No cracks	4.50
24	No cracks	5.00
25	Failure	–

Table 14: Results of Simulated Tendon Load on Fiberglass Rib

C Additional Figures and AI Prompts

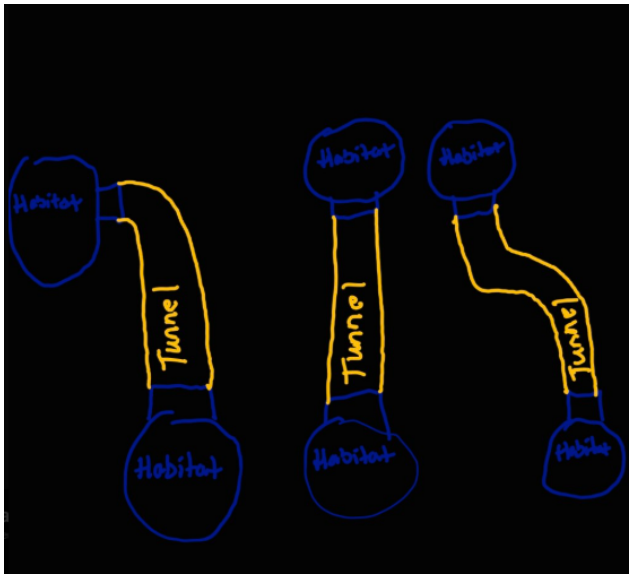

Figure 27: Original tunnel pathing diagram before AI enhancement

This Picture was uploaded into Chat GPT and used this prompt to enhance the quality and design.“Can you make this into a realistic diagram with the tunnels being from chats we’ve previously talked about?” “Can you recreate this image but with the system on the right can you make the curve more smooth like an s instead of jagged?”

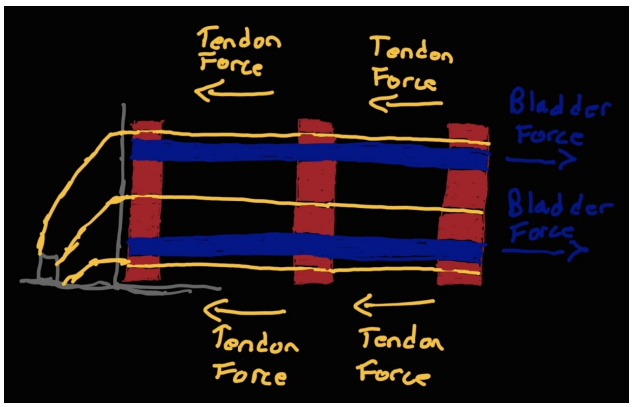

Figure 28: Original tendon force diagram before AI enhancement

This Picture was uploaded into Chat GPT and used this prompt to enhance the quality and design. “Can you make this into a cleaner diagram?”

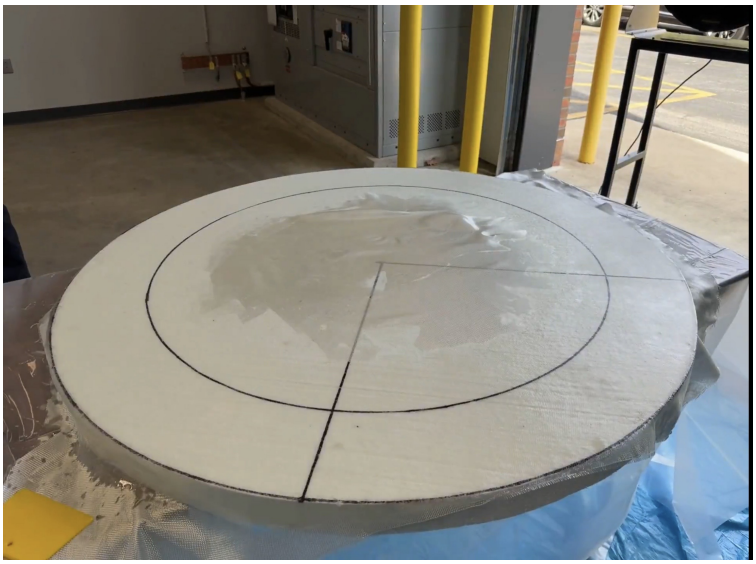

Figure 29: White Foam Fiberglass Layup

This picture shows part of the fiber glass layup process. This 3” thick white foam had the support rib drawn onto the face of the foam, epoxy was spread around the rib, a fiberglass sheet was placed down, more epoxy was added, using a small squeegee at a low angle, the epoxy was spread and left to dry.

Figure 30: Prototype Frame Assembly

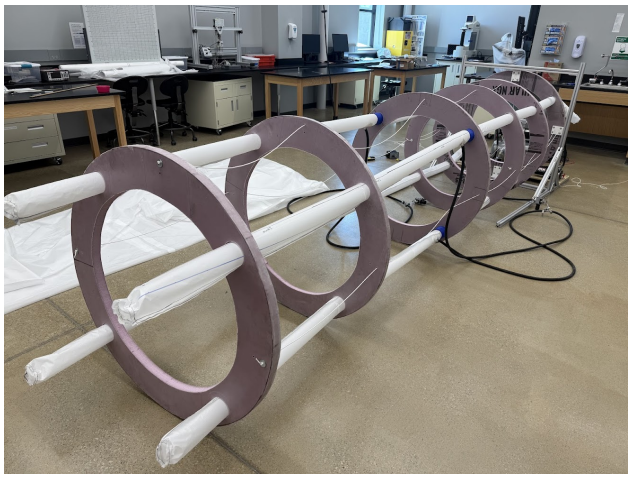

Figure 31: Prototype tunnel assembly before placement of outer shell.

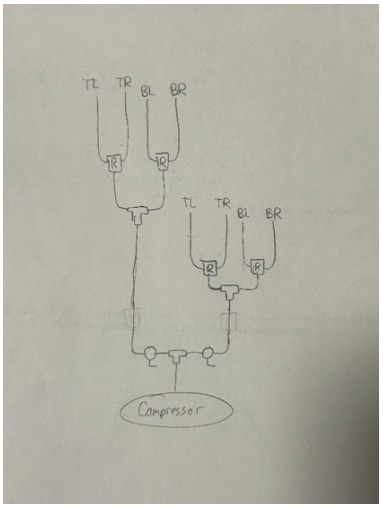

Figure 32: Original air intake diagram before AI enhancement

This Picture was uploaded into Chat GPT and used this prompt to enhance the quality and design. “Can you make this into a cleaner diagram.”